A Double Leucine within the GLUT4 Glucose Transporter COOH-Terminal Domain Functions as an Endocytosis Signal

Silvia Corvera,* Anil Chawla, Ranjan Chakrabarti, Marguerite Joly,* Joanne Buxton, and Michael P. Czech

Program in Molecular Medicine and Departments of Biochemistry and Molecular Biology, and *Cell Biology, University of Massachusetts Medical Center, Worcester, Massachusetts 01605

Abstract. The unique COOH-terminal 30-amino acid region of the adipocyte/skeletal muscle glucose transporter (GLUT4) appears to be a major structural determinant of this protein's perinuclear localization, from where it is redistributed to the cell surface in response to insulin. To test whether an underlying mechanism of this domain's function involves glucose transporter endocytosis rates, transfected cells were generated expressing exofacial hemagglutinin epitope (HA)-tagged erythrocyte/brain glucose transporter (GLUT1) or a chimera containing the COOH-terminal 30 amino acids of GLUT4 substituted onto this GLUT1 construct. Incubation of COS-7 or CHO cells expressing the HA-tagged chimera with anti-HA antibody at 37° resulted in an increased rate of antibody internalization compared to cells expressing similar levels of HA-tagged GLUT1, which displays a cell surface disposition. Colocalization of the internalized anti-HA antibody in vesicular structures with internalized transferrin and with total transporters was established by digital imaging microscopy, suggesting the total cellular pool of transporters are continuously recycling through the coated pit endocytosis pathway. Mutation of the unique double leucines 489 and 490 in the rat GLUT4 COOH-terminal domain to alanines caused the HA-tagged chimera to revert to the slow endocytosis rate and steady-state cell surface display characteristic of GLUT1. These results support the hypothesis that the double leucine motif in the GLUT4 COOH terminus operates as a rapid endocytosis and retention signal in the GLUT4 transporter, causing its localization to intracellular compartments in the absence of insulin.

EXPERIMENTS reported over the last four decades have clearly defined the stimulatory effect of insulin on membrane transport of glucose as a key aspect of this hormone's physiological function. This acute action of insulin is maximal within a few minutes, leads to over tenfold increases in hexose influx rates, and is largely restricted to muscle and fat cells in vivo (8, 32). Using fat cell fractionation techniques, it was shown that insulin-stimulated glucose uptake is associated with a rapid redistribution of functional glucose transporters from an intracellular membrane fraction to plasma membranes (5, 35). Subsequently, direct demonstration of the rapid increase in glucose transporter proteins on the cell surface of intact cells in response to insulin has been accomplished using transporter affinity labeling (16, 20, 28) and trypsin cleavage (6) techniques, immunoelectron microscopy (33, 34), and an antibody binding assay using an epitope-tagged glucose transporter construct (24). In addition, a cloned (2, 4, 10, 19, 23) insulin-regulated glucose transporter isoform denoted as GLUT4 was shown to be expressed exclusively in fat and muscle cells, and accounts for most of the increased transporter protein recruited to the plasma membrane by insulin (40). A second glucose transporter isoform denoted as GLUT1 is present in primary insulin-sensitive cells at a much lower concentration than GLUT4. Despite substantial sequence similarity with GLUT4, GLUT1 displays a predominantly cell surface localization even in the absence of insulin (15, 40).

The distinct differences in the cellular localization of GLUT1 and GLUT4 has allowed microscopic and biochemical analysis of GLUT1/GLUT4 chimera transporters to identify regions of GLUT4 that confer its intracellular disposition. Our laboratories recently engineered a number of such chimera cDNA constructs with an insert encoding the hemagglutinin (HA)[1] epitope YPYDVPDYA positioned in the major exofacial loop of the transporter protein structure (7). Binding of a monoclonal anti-HA antibody to intact cells expressing these HA-tagged constructs permits quantitative

Address all correspondence to Drs. Michael P. Czech or Silvia Corvera, Program in Molecular Medicine, University of Massachusetts Medical Center, 373 Plantation Street, Worcester, MA 01605.

1. *Abbreviations used in this paper*: GLUT4, adipocyte/skeletal muscle glucose transporter; GLUT1, erythrocyte/brain glucose transporter; HA, hemagglutinin epitope.

analysis of the transporter protein levels present on the cell surface. Such analysis in transfected COS-7 and CHO cells revealed the 30-amino acid COOH-terminal domain of GLUT4 confers a strong intracellular localization signal when substituted onto the GLUT1 transporter protein. Conversely, a chimera containing the 29 residue COOH terminus of GLUT1 substituted onto exofacial epitope-tagged GLUT4 resulted in a predominant cell surface distribution. Similar results have now been reported in cultured PC-12 cells (17) and frog oocytes (26) expressing GLUT1/GLUT4 chimera transporter proteins. Although other GLUT4 domains have also been reported to be important in determining its characteristic perinuclear localization (1, 29, 30), the combined data from three laboratories now strongly support a major role of the 30-amino acid GLUT4 COOH terminus (7, 17, 26).

The experimental documentation that a major intracellular localization signal in the GLUT4 protein resides in its COOH terminus raises the hypothesis that this structure interacts with one or more cellular components involved in cellular membrane trafficking of GLUT4. An important advantage of the exofacial HA epitope-tagged glucose transporter proteins is that their cellular internalization rates can be quantified by monitoring the uptake of anti-HA antibody added to intact cells expressing these constructs. The aim of the present work was to determine whether the GLUT4 COOH-terminal domain contains endocytic targeting properties by exploiting this unique feature of the HA-tagged transporter proteins. The experiments reported here demonstrate a striking enhancement of exofacial HA epitope-tagged GLUT1 endocytosis when the GLUT4 COOH-terminal 30 amino acids are substituted for the corresponding GLUT1 COOH terminus. Furthermore, we demonstrate a requirement for an intact double leucine motif in this GLUT4 COOH-terminal region to confer the rapid endocytosis rate. The data suggest an important role for the coated pit-mediated endocytosis pathway in the steady-state intracellular disposition of the GLUT4 transporter protein.

Materials and Methods

Cell Culture

COS-7 and CHO-K1 cells were obtained from American Type Culture Collection (Rockville, MD). Media, trypsin, antibiotics, and G418 were from GIBCO/BRL (Gaithersburg, MD), and FBS was purchased from Upstate Biotechnology, Inc. (Lake Placid, NY). COS-7 cells were maintained in DME with 10% FBS, 50 U/ml penicillin, and 50 μg/ml streptomycin in a 37°C humidified CO_2 incubator. The cells were subcultured before reaching confluence. CHO-K1 cell lines were maintained in Ham's F-12 medium with 10% FBS, 50 U/ml penicillin, and 50 μg/ml streptomycin in a 37°C humidified CO_2 incubator.

Construction of HA-tagged Chimera Transporters

The construction of GLUT1X and 1(1-462)/4 was described previously (7). The construct 1(1-462)/4LL was made in the following manner. Oligonucleotides corresponding to the amino acids 480-509 of GLUT4 containing the mutations to change L489 and L490 to alanine residues were synthesized. The double stranded oligonucleotide fragment was cloned into the BglII-SalI site of the original 1(1-462)/4 construct in pUC19. The mutated construct was then transferred to the expression vector pCMV5. Construct 1(1-462)/4Y was made by truncating the original 1(1-462)/4 construct at amino acid 503 in the following way. A double stranded oligonucleotide corresponding to amino acids 480-503 of GLUT4 was inserted at BglII and SalI of the original 1(1-462)/4 construct in pUC19. The new construct was transferred to pCMV5.

Transient Expression of HA-Epitope-tagged Chimera Transporter cDNAs in COS-7 Cells

COS-7 cells were seeded at 100,000 cells per 22-mm round, glass coverslip and transfection of HA-epitope-tagged chimera transporter cDNAs was performed by the calcium phosphate precipitation method as described (11). Cells were analyzed by immunofluorescence 48 h later.

Stable Expression of Chimera Transporter cDNAs in CHO-K1 Cells

Subconfluent CHO-K1 cells were cotransfected with pRSVneo and chimera transporter cDNA by the calcium phosphate method described. G418-resistant colonies were picked up with the use of cloning cylinders and expanded. Positive cell lines were identified using immunofluorescence with anti-HA or anti-GLUT4 antibodies. Expression was confirmed by Western blotting of total cellular membranes.

Immunofluorescence of Transfected Cells

Forty-eight hours after transfection, COS-7 cells were washed three times in PBS (171 mM NaCl, 10 mM Na_2HPO_4, 3.3 mM KCl, 1.8 mM KH_2PO_4), fixed for 10 min at room temperature in 4% formaldehyde in PBS, and rewashed three times in PBS. The fixed cells were then incubated with PBS containing 1% FBS and anti-HA antibody (mouse monoclonal 12CA5, BAbCO, Berkeley, CA) diluted 1:1,000, for 2-3 h at room temperature. The cells were washed and exposed to FITC-coupled goat anti-mouse IgG for 30 min at room temperature. After washing, the cells were postfixed with 4% formaldehyde in PBS for 5 min at room temperature. Cells were then permeabilized by incubating with PBS containing 1% FBS and 0.5% Triton X-100 for 30 min at room temperature. Cells were then incubated with a 1:1,000 dilution of either rabbit anti-GLUT4 IgG (R1288) or monoclonal anti-HA antibody (12CA5) depending on the COOH-terminal structure of the chimera for 18 h at 4°C. The cells were then again washed, and exposed to a 1:1,000 dilution of rhodamine-coupled goat-anti-rabbit or anti-mouse IgG (Tago, Inc., Burlington, CA). The cells were thoroughly washed and the coverglasses were mounted on slides in 90% glycerol + 2.5% DABCO.

CHO-K1 cell lines were analyzed by immunofluorescence essentially as described above, except that the cells on coverslips were permeabilized directly after fixation and total cellular staining was detected with anti-HA antibody and anti-GLUT4 antibody (R1288). Primary antibodies were detected with FITC-conjugated goat anti-mouse and rhodamine-conjugated goat anti-rabbit second antibodies as above.

Iodination of HA Antibody

Monoclonal antibody (12CA5) was purchased from BAbCO and the IgG fraction was purified. 75 μg of the anti-HA IgG was iodinated using a lactoperoxidase kit (ICN) according to manufacturer's instructions.

Iodinated Antibody Uptake

Cells were grown to 80% confluence in 24 well dishes. Cells were equilibrated in buffer A (serum-free F12 media) for 30 min at 37°C. The buffer was then replaced with ice-cold buffer A containing 30 μg/ml anti-HA IgG and 10^6 cpm of ^{125}I-anti-HA IgG. The plates were incubated at 4°C for 1 h, and then washed several times with ice-cold buffer A. The cells were then incubated with buffer A at 37°C for 2-10 min. Surface bound antibody was eluted in two sequential two minute washes with acidic buffer (100 mM Glycine, 20 mM Magnesium Acetate, 50 mM Potassium Chloride, pH 2.2). The two washes were saved and pooled, and cell monolayers were solubilized in 1% SDS. The radioactivity present in the acid labile and resistant pools was measured by gamma counting.

Antibody Uptake Detected with Immunofluorescence

Cells grown on glass coverslips were equilibrated at 37°C for 30 min in buffer A. The buffer was aspirated and replaced with fresh buffer A containing 30 μg/ml anti-HA IgG for 10 or 60 min. The cells were then washed two times for 2 min each with ice cold acidic buffer as above, and then washed with ice cold PBS and fixed in 4% formaldehyde for 10 min. The cells were permeabilized for 1 min in room temperature methanol and briefly air dried. The fixed cells were incubated in PBS + 1% FBS for 15 min, and then incubated with a 1:1,000 dilution of FITC-coupled anti-mouse secondary antibody in the same buffer for 30 min. After several washes with PBS + 1% FBS, the cells were postfixed in 4% formaldehyde

for 10 min. Total expressed transporter was detected with a 1:1,000 dilution of anti-HA or anti-GLUT4 (R1288) antibody, washed in PBS + 1% FBS, and bound antibodies detected with a 1:1,000 dilution of Rhodamine coupled anti-mouse (anti-HA) or anti-rabbit (GLUT4). After extensive washes with PBS + 1% FBS, the coverslips were mounted on slides using 90% glycerol + 2.5% DABCO.

Antibody and Transferrin Uptake

Cells grown as described above were assayed similarly except that 2.5 μg/ml Texas red-labeled transferrin was included in the incubation. Internalized antibody was detected with FITC-coupled anti-mouse antibody as above. Total expression was not measured in these experiments.

2-Deoxyglucose Uptake

Cells were assayed for 2-deoxyglucose uptake as described previously (13). Nonspecific uptake, measured in the presence of 20 μM cytochalasin B and 300 μM phloretin, was subtracted and the cpm were normalized per 10^5 cells.

Digital Imaging Microscopy

Samples were visualized on a Zeiss IM-35 microscope using a Nikon Apo 60/1.4 oil immersion lens and an 8X eyepiece. Two-dimensional images were recorded using a thermoelectrically cooled charge-coupled device camera (Photometrics Ltd., Tucson, AZ). To determine colocalization of signals, a powerful deconvolution algorithm that reverses the blurring introduced by the microscope optics was used. For these experiments, 30 serial two-dimensional images were recorded at 0.25 μm intervals. Each image was corrected for lamp intensity variations and photobleaching. Blurring of fluorescence from regions above and below the plane of focus was reversed using an iterative constrained deconvolution algorithm based on the theory of ill-posed problems.

Results

To further define the role of the GLUT4 COOH-terminal 30-amino acid domain as a signal for intracellular localization, the present studies focused on glucose transporter chimeras in which this GLUT4 COOH-terminal domain is substituted onto GLUT1 (Fig. 1 *A*). The chimera denoted 1(1-462)/4 contains native sequences of human GLUT1 (residues 1-462) and the rat GLUT4 COOH terminus (residues 480-509), and has previously been shown to display a GLUT4-like perinuclear disposition when expressed in COS-7 or CHO cells (7). Under similar experimental conditions, native GLUT1 is primarily a cell surface protein. In comparing the amino acid sequences of the GLUT1 and GLUT4 COOH-terminal regions (Fig. 1 *B*), two motifs unique to GLUT4 were noteworthy based on studies related to membrane trafficking of other proteins. Double leucine motifs present in many membrane receptors (21, 22, 25, 27, 31, 37) are required for normal movements through membrane compartments, while tyrosine residues in juxtamembrane domains have been implicated in receptor endocytosis (18, 25, 36). These considerations led us to engineer mutant chimera constructs in which the double leucines 489 and 490 were converted to alanines (construct 1(1-462)/4LL) or the GLUT4 COOH terminus was truncated at position 503 so that tyrosine 504 is missing (construct 1(1-462)/4Y). Additionally, each of the constructs depicted in Fig. 1 *A* were engineered to contain the HA epitope sequence YPYDVPDYA within the major exofacial loop. The native chimera (1(1-462/4) and double leucine mutant (1(1-462)/4LL) constructs depicted in Fig. 1 encode functional transporter proteins because their overexpression in stably transfected CHO cells confers severalfold increases in glucose transport activity to these cell lines (data not shown).

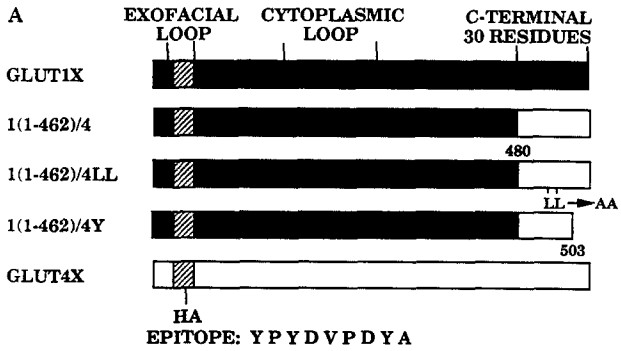

B

rGLUT4C 480 S A T F R R T P S L L K V E Q E P S T E L G

hGLUT1C I A S G F R Q G G A S Q S D K T P E E L F H

rGLUT4C P L Y E P E N D 509

hGLUT1C P L G A D S Q V

Figure 1. HA epitope-tagged chimeras and mutant chimeras and their comparison to the full length GLUT1 and GLUT4 transporters. The location of the HA epitope-tag insert (IDYPYDVPDYA) in the exofacial loop is indicated by the hatched area. This epitope is inserted after amino acid 53 in all transporters except GLUT4X in which the HA sequence is inserted after amino acid 83. GLUT1X and GLUT4X contain the entire sequence of the appropriate isoform. The construct 1(1-462)/4 contains the first 462 amino acids of GLUT1 and the last 30 amino acids of GLUT4. For 1(1-462)/4LL, the leucines indicated by asterisks in *B* have been mutated to alanine residues. Construct 1(1-462)/4Y is truncated at amino acid number 503 so that the tyrosine at position 504 and the rest of the molecule is missing.

GLUT4 Perinuclear Localization Requires the COOH-Terminal Dileucine

To determine the steady-state cellular localization of native and mutant glucose transporter chimeras, the exofacial HA-tagged constructs depicted in Fig. 1 *A* were transiently expressed in COS-7 cells (Fig. 2). The cell surface concentration of each construct was analyzed by immunofluorescence microscopy of non-permeabilized cells using a monoclonal anti-HA epitope antibody (12CA5) followed by a FITC-coupled anti-mouse immunoglobulin secondary antibody. Subsequently, the cellular localization of all expressed transporters in the same cells was determined by permeabilization with 0.5% Triton, an exposure to anti-GLUT4 or anti-HA antibody, and then incubation with a rhodamine-coupled anti-rabbit or anti-mouse immunoglobulin secondary antibody. That this procedure quantifies the cell surface complement of expressed transporters was previously verified by the finding that exofacial HA-tagged GLUT1, but not GLUT1 tagged at its cytoplasmic NH_2-terminus, was readily detected by anti-HA antibody bound to nonpermeabilized cells (7).

Fig. 2 shows that at similar levels of cellular expression, much higher levels of GLUT1X are detected at the cell surface compared to the 1(1-462)/4 construct, confirming our previous findings that the GLUT4 COOH terminus confers an intracellular disposition. The marked perinuclear appearance of the 1(1-462)/4 chimera visualized in permeabilized cells (*upper panel*) resembles the results obtained with native GLUT4 (not shown, see references 7, 17, 26, 29). Similar data are obtained when the 1(1-462)/4Y protein is ex-

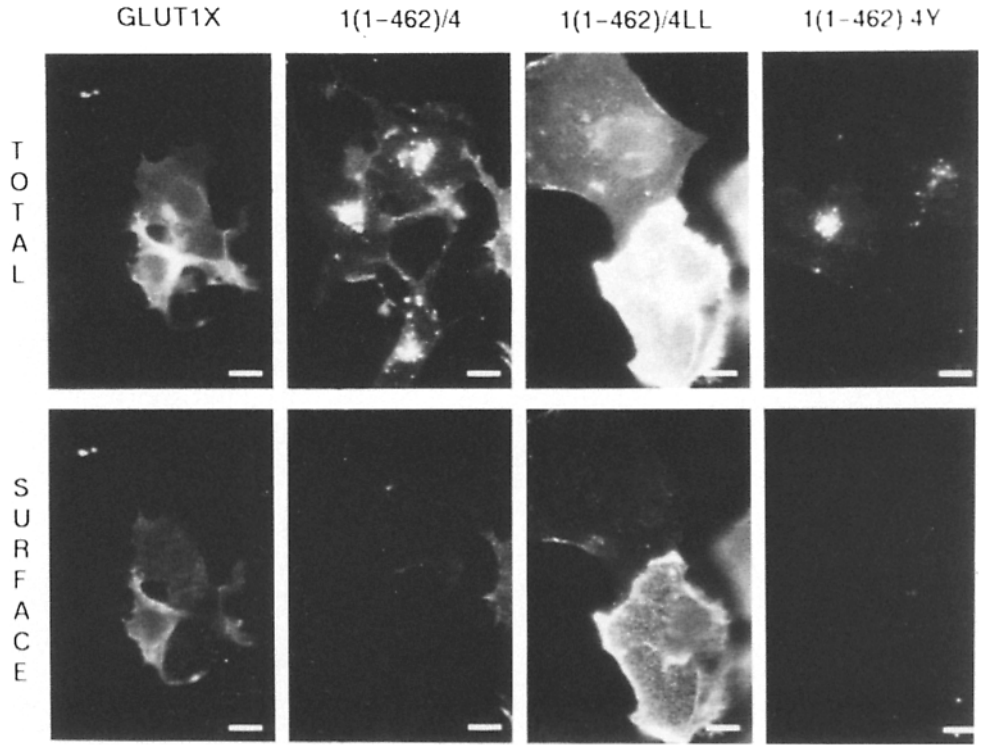

Figure 2. Immunofluorescence microscopy of HA-tagged transporter constructs transiently expressed in COS-7 cells. COS-7 cells were fixed in 4% formaldehyde 48 h after transfection with the indicated constructs. Transporters present at the cell surface (*SURFACE*) were detected with anti-HA antibody (12CA5) and FITC-conjugated anti-mouse second antibody before permeabilizing the cells. The cells were permeabilized and total transporter expression (*TOTAL*) was detected with anti-HA (for *GLUT1X*) or anti-GLUT4 (*RI288*) (for chimeras) antibody and rhodamine-coupled anti-mouse (for anti-HA) or anti-rabbit (for anti-GLUT4) second antibody. To accurately quantify the proportion of each transporter present at the cell surface of translocated cells, the fluorescence intensity (Rhodamine and FITC) of all transfected cells found in 10 fields (10–15 cells) for each construct was measured. The ratios of surface/total fluorescence obtained were expressed as mean ± SEM, and were 0.51 ± 0.08, 0.18 ± 0.05, and 0.51 ± 0.10 for GLUT 1X, 1(1-462)/4 and 1(1-462)/4LL, respectively. Bar, 10 μm.

pressed in COS-7 cells. In contrast, at equal levels of expression, mutation of the double leucines in this construct to alanines (construct 1(1-462)/4LL in Fig. 1 *A*) results in a large increase in the levels of transporter at the cell surface, as visualized by the intense signal from anti-HA antibody in nonpermeabilized cells (Fig. 2, *lower cell in lower panel*), similar to GLUT1X. In permeabilized cells this mutant construct is distributed throughout the cell rather than restricted to the perinuclear region, again similar to the GLUT1X transporter protein (Fig. 2). Quantifications of the immunofluorescence intensities by digital image microscopy to obtain surface transporter content/total transporter ratios found in 10 fields each (10–15 cells) for GLUT1X, 1(1-462)/4 and 1(1-462)/4LL yielded the values of 0.51 ± 0.08, 0.18 ± 0.05, and 0.51 ± 0.10, respectively. Taken together, these data indicate that the capability of the GLUT4 COOH terminus to confer a steady-state intracellular localization when substituted onto the GLUT1X construct requires intact leucines 489 and 490.

The validity of this conclusion was tested using independent methodology in a different cell type. As depicted in Fig. 3, CHO cells stably transfected with GLUT1X, 1(1-462)/4 or 1(1-462)/4LL were fixed, permeabilized, and analyzed with anti-HA antibody and an anti-GLUT4 COOH-terminal peptide antibody. GLUT1X protein exhibited a dispersed pattern of anti-HA immunoreactivity, with high intensity at cell borders characteristic of its cell surface concentration. As expected, these same cells were devoid of anti-GLUT4 antibody-mediated immunofluorescence (Fig. 3, *top panel*). In sharp contrast, the chimera containing the native GLUT4 COOH-terminal region was largely restricted to a perinuclear localization when permeabilized cells were probed with either anti-HA (*lower panel*) or anti-GLUT4 (*top panel*) antibodies. Again, mutation of the double leucines 489 and 490 to alanines caused reversion of this distribution to a GLUT1X-like, cell surface phenotype, as evidenced by probing with either antibody (Fig. 3). Quantification of data obtained from other experiments on CHO cells (not shown) for SURFACE/TOTAL values also confirmed similarly increased cell surface content of GLUT1X and 1(1-462)/4LL over 1(1-462)/4. These data demonstrate that the double leucine motif is a necessary element of the cellular localization signal in the GLUT4 COOH terminus.

The GLUT4 COOH-Terminal Dileucine Signals Rapid Endocytosis

In the next series of experiments, we took advantage of the fact that anti-HA antibody binds to exofacial-tagged transporter proteins in intact living cells. The ability of HA-tagged transporters to direct the internalization of antibody can be used as a direct means of estimating transporter endocytosis. Transiently transfected COS-7 cells (Fig. 4) and stably transfected CHO cells (Fig. 5) expressing GLUT1X, chimera 1(1-462)/4, or the double leucine mutant chimera 1(1-462)/4LL were incubated with 12CA5 antibody at 37° for 10 or 60 min. Cells were then fixed, permeabilized, and incubated with FITC-labeled anti-mouse immunoglobulin antibody to visualize the internalized monoclonal 12CA5 (panels labeled "10 min" and "60 min" in Figs. 4 and 5). Distribution of total transporter proteins in the same fixed permeabilized cells were visualized by a subsequent incubation with anti-HA (for GLUT1X) or anti-GLUT4 (for chimeras) followed by rhodamine-conjugated anti-mouse or anti-rab-

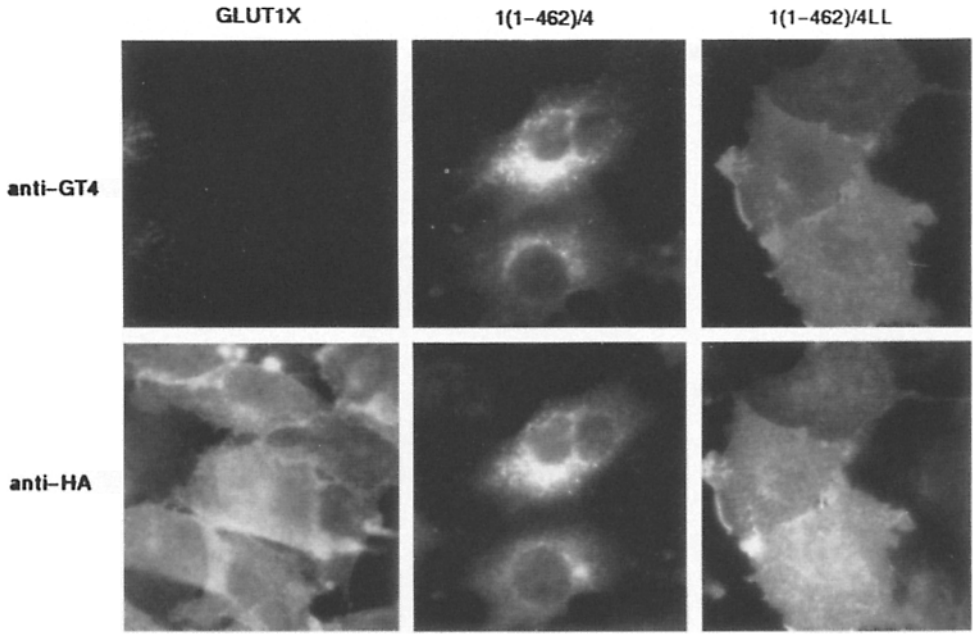

Figure 3. Immunofluorescence microscopy of CHO cells expressing GLUT1X, 1(1-462)/4, and 1(1-462)/4LL. CHO cells expressing the indicated chimeras were fixed in 4% formaldehyde and permeabilized. Immunoreactivity with anti-HA (*lower panels*) and anti-GLUT4 (R1288) antibodies (*upper panels*) was detected with FITC-coupled anti-mouse and rhodamine-coupled anti-rabbit antibodies, respectively. Bar, 10 μm.

bit immunoglobulin antibody (panels labeled "total" above the 10 min or 60 min panels, respectively). Time-dependent uptake of the anti-HA antibody directed by the glucose transporter proteins was observed in both COS-7 (Fig. 4) and CHO (Fig. 5) cells, but was much more pronounced with cells expressing the 1(1-462)/4 chimera compared to GLUT1X or the double leucine mutant chimera. In COS-7 cells, 12CA5 antibody uptake in GLUT1X or 1(1-462)/4LL expressing cells was virtually undetectable at 10 min, while the 1(1-462)/4 chimera mediated a relatively strong signal by this time (Fig. 4). By 60 min of incubation, cells expressing the 1(1-462)/4 chimera exhibited intense accumulation of the 12CA5 antibody in the perinuclear region as well as in punctate, peripheral structures. Mutation of the double leucines in this chimera abolished detectable uptake of the anti-HA antibody into the perinuclear region. No internalized antibody could be detected in non-transfected cells (not shown).

The significantly elevated rates of 1(1-462)/4 protein inter-

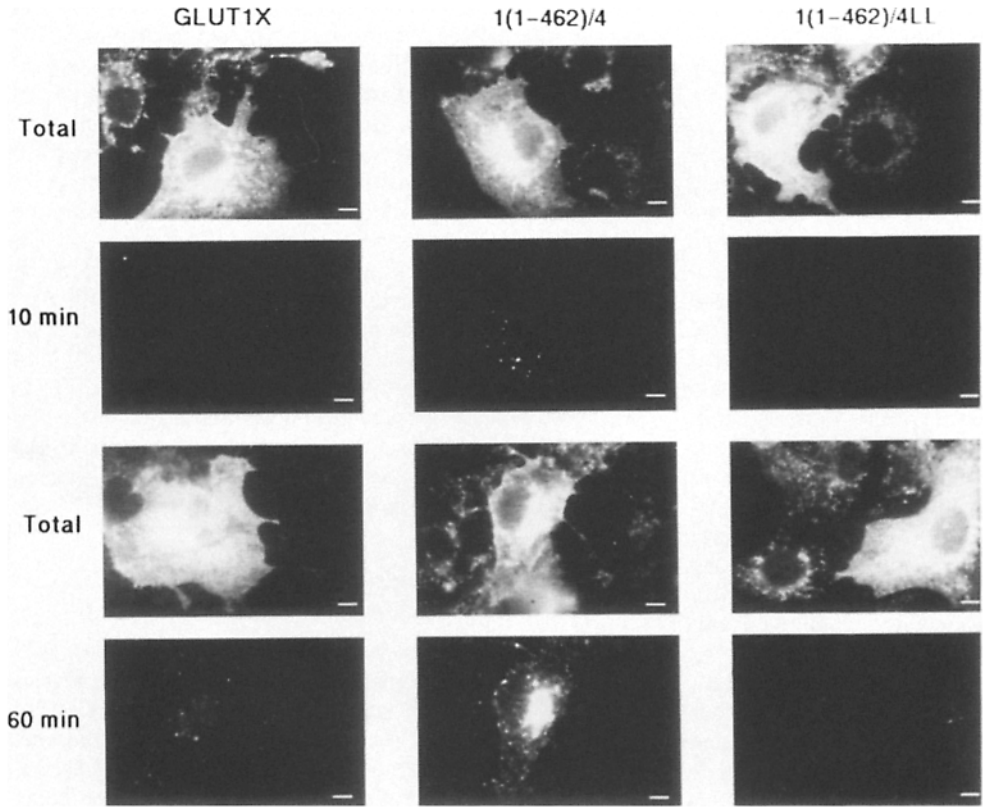

Figure 4. Anti-HA antibody internalization in COS-7 cells transiently expressing HA-tagged transporter chimeras. 48 h after transfection with the indicated constructs, cells were incubated at 37°C with anti-HA IgG for 10 min (*upper panels*) or 60 min (*lower panels*). Cell surface antibody was released by washing two times for 2 min each with ice cold acidic buffer. Cells were then washed with PBS on ice, fixed in 4% formaldehyde, and permeabilized. Internalized antibody was detected with FITC-conjugated anti-mouse antibody. Total transporter expression (*TOTAL*) was analyzed as indicated in the legend of Fig. 2. Bar, 10 μm.

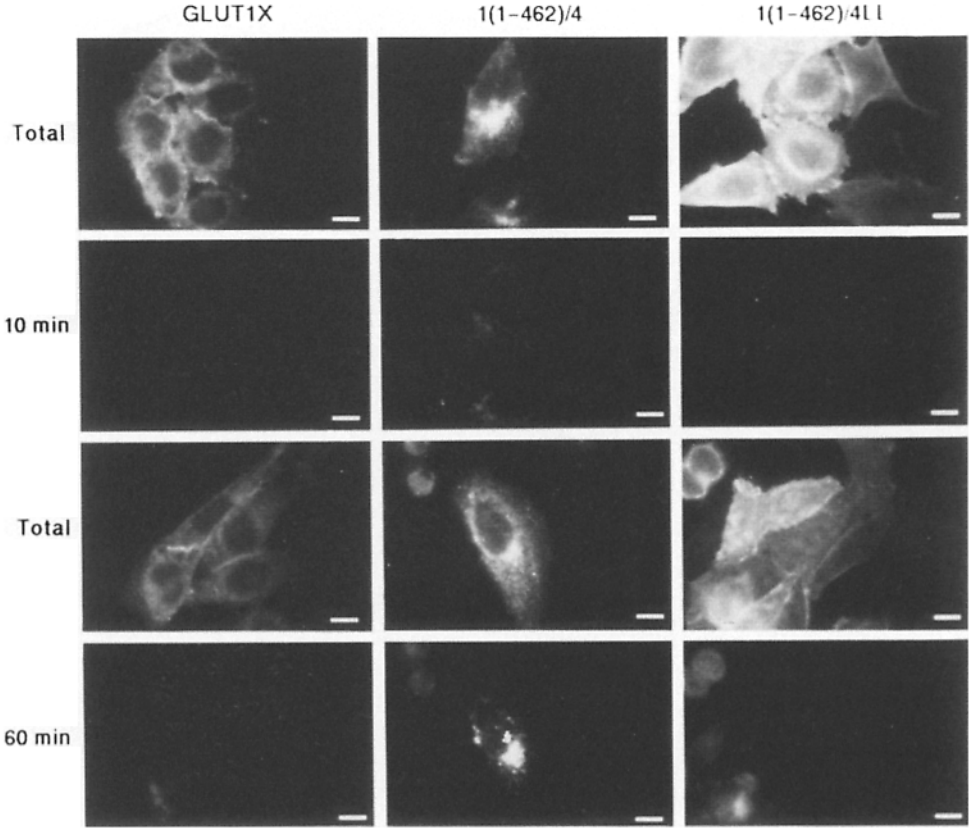

Figure 5. Anti-HA antibody internalization in CHO cells expressing HA-tagged transporter chimeras. CHO cells expressing the indicated transporters were incubated at 37°C with anti-HA IgG for 10 min (*upper panels*) or 60 min (*lower panels*). Cells were washed on ice, fixed in 4% formaldehyde, and permeabilized. Internalized antibody was detected with FITC-conjugated anti-mouse antibody. Total transporter expression (*TOTAL*) was analyzed as indicated in the legend of Fig. 2. Bar, 10 μm.

nalization observed in Figs. 4 and 5 relative to those of GLUT1X and the mutant 1(1-462)/4LL chimera seemed particularly remarkable because much less of the former chimera protein is present on the cell surface at steady-state compared to the latter proteins (Fig. 2). Thus, a much smaller pool of surface bound 12CA5 antibody is available to be internalized in cells expressing the 1(1-462)/4 chimera compared to those expressing GLUT1X or 1(1-462)/4LL (Fig. 1), even though in fact the former cells do internalize more 12CA5 antibody than the latter (Figs. 4 and 5). Using digital imaging microscopy, the fluorescence intensity associated with the newly internalized anti-HA antibody in COS-7 cells was quantified. When normalized to the calculated cell surface content of transporter protein, we obtained internalization values (anti-HA Uptake/Steady-state Cell Surface Transporter Content) for 1(1-462)/4 that were three times greater than GLUT1X and 1(1-462)/4LL at 10 min and over 10-fold greater at 60 min. Experiments were also conducted to quantify the 12CA5 antibody internalization rate relative to its steady-state cell surface binding using methodology previously established for comparison of receptor endocytosis rates (9). Antibody 12CA5 labeled with ^{125}I was incubated with stably transfected CHO cells expressing transporter proteins GLUT1X, 1(1-462)/4 or 1(1-462)/4LL for 1 h at 4° to bind cell surface transporters. Unbound antibody was washed away and cells were incubated at 37° for various times (2–10 min) to allow endocytosis to proceed. The amount of 12CA5 antibody remaining on the cell surface at each time point was removed by acid washing, and quantified. The amount of internalized radioactivity still associated with the cells was also determined.

The data obtained for each time of internalization in these experiments was plotted as a ratio of internalized 12CA5 antibody to cell surface bound antibody (In/Sur) in Fig. 6. About half of the initial surface bound 12CA5 antibody was already internalized within only two min of incubation at 37° when directed by the 1(1-462)/4 transporter chimera, and internalization continued to proceed rapidly through the 10 min incubation period. In contrast, the In/Sur ratio calculated for the GLUT1X containing cells was about twofold lower at 2 min and fivefold lower at the 10 min time point (Fig. 6). Cells expressing the mutant chimera with the double leucines converted to alanines displayed a low internalization rate indistinguishable from that measured in GLUT1X-expressing cells. Taken together, the data presented in Figs. 4–6 demonstrate that the steady-state perinuclear localization conferred by the 30 residue GLUT4 COOH-terminal domain when substituted onto GLUT1 is associated with an elevated rate of internalization compared to native GLUT1. Both of these functions are directed by the GLUT4 COOH terminus, and are abolished upon mutation of the double leucine motif in the GLUT4 domain.

Newly Internalized and Total Cellular Chimera Transporters Colocalize

The results described above indicate that the GLUT4 COOH terminus contains a signal for internalization, and suggests that the predominantly intracellular localization of GLUT4 is the result of efficient retrieval from the plasma membrane. However, an alternative possibility could be that GLUT4 is targeted to two different cellular compartments, one being

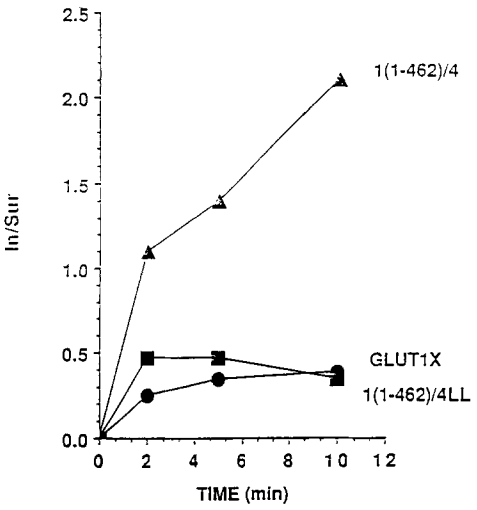

Figure 6. Antibody internalization initial rate determinations from CHO cells expressing GLUT1X, 1(1-462)/4, and 1(1-462)/4LL. CHO cells expressing the indicated constructs were incubated at 4°C for 60 min with ^{125}I HA IgG and washed on ice. The cells were then incubated at 37°C for 2, 5, or 10 min. After washing, the surface bound antibody was released using acidic buffer and counted. The cells were solubilized, and internalized counts were determined. The cpm were corrected for cell number. The ratio of internalized counts to surface counts (*IN/SUR*) was determined and plotted vs time for each cell line.

the endocytic pathway, and another being a specialized intracellular storage pool which keeps the transporter sequestered from the plasma membrane. To determine whether the pool of transporters that internalize antibody is separated from a non-recycling pool, we used digital imaging microscopy to assess rigorously the degree of colocalization of recycling vs total cellular pools of transporters. Transfected COS-7 cells producing 1(1-462)/4 chimera protein were incubated with the anti-HA antibody for 60 min followed by acid washing, fixation, permeabilization, and probing with FITC-anti-mouse immunoglobulin antibody. After this treatment, the same cells were incubated with anti-GLUT4 antibody followed by rhodamine-labeled anti-rabbit immunoglobulin antibody to visualize the cellular distribution of the total pool of chimera transporter proteins. Three dimensional images of the total pool of transporters (two representative fields visualized in red in *left panels* of Fig. 7) and of the fluorescein signal associated with transporters internalized during the 60 min incubation (visualized in green in the *middle panels* of Fig. 7) were generated. Areas of colocalization of rhodamine-based and fluorescein-based signals observed after overlapping both images are displayed in white (*right panels* of Fig. 7).

Three important findings emerge from this analysis: First, the 1(1-462)/4 chimera protein in these cells appears as a distinct punctate pattern, suggesting its sorting into discrete vesicular structures (*left panels*). Second, while many of these chimera-containing structures are situated in the perinuclear region of the cells, they are clearly present throughout the cytoplasm. Third, newly internalized 1(/1-462)/4 chimera proteins distributed within 60 min to most of the same vesicular structures that contain the bulk transporter protein pool (*right panels* of Fig. 7). These data are consistent with the hypothesis that most if not all of the 1(1-462)/4 chimera transporters are continually recycling between intracellular vesicular structures and the cell surface membrane in COS-7 cells.

Newly Internalized Chimera Transporters and Transferrin Colocalize

The efficient endocytosis of 1(1-462)/4 chimera transporter proteins demonstrated by the present work is consistent with morphological (30) and biochemical (3) evidence that significant amounts of GLUT4 is present in clathrin-coated membrane structures. We tested whether the 1(1-462)/4 chimera is internalized via the endocytic pathway through which transferrin receptor and other receptors are internalized. COS-7 cells expressing 1(1-462)/4 chimera were incubated simultaneously with Texas red-tagged transferrin and anti-HA antibody for 60 min at 37°C. Cells were acid washed, fixed, permeabilized, and primary 12CA5 antibody was detected with FITC-labeled anti-mouse immunoglobulin antibody. The same three dimensional reconstruction and colocalization of Texas red vs fluorescein-based fluorescence analysis were performed as described above for Fig. 7. The data in Fig. 8 depicting two distinct fields (*upper* vs *lower panels*) show quite similar distribution profiles for the internalized transferrin (visualized in red in *left panels*) and anti-HA antibody (visualized in green in *middle panels*). Note that in the upper panels a single cell is visualized, whereas in the lower panels, multiple cells are present. Only one cell among the latter has been transfected with the chimera transporter cDNA, whereas all the cells contain endogenous transferrin receptors and internalized Texas red-labeled transferrin. Numerous vesicular structures harboring internalized transferrin also contain chimera transporter protein, as visualized in white in the right panels of Fig. 8.

Discussion

The GLUT4 COOH Terminus Confers a Rapid Endocytosis Rate

Recent work has led to a consensus among several groups (7, 17, 26) that cytoplasmic sequences in the GLUT4 COOH terminus play a major role in the predominant perinuclear localization of the GLUT4 transporter protein observed in many cell types. We have previously reported that an exofacial HA-tagged GLUT1/GLUT4 chimera containing the 30 residue GLUT4 COOH terminus displays a predominantly intracellular localization when expressed either in COS-7 or CHO cells (7). A primary focus of the present studies was to examine the cellular trafficking properties of the GLUT4 COOH terminus that influence its subcellular distribution. A key finding reported here is that expression of the 1(1-462)/4 chimera caused a pronounced intracellular accumulation of anti-HA antibody added to the cell culture medium. The accumulation mediated by the 1(1-462)/4 chimera was much greater than that mediated by GLUT1 (Figs. 4–6). These data suggest that a mechanism involving rapid retrieval from the cell surface may account for the intracellular localization of chimeras containing the GLUT4 COOH terminus.

Several independent experiments further reinforce the conclusion that the GLUT4 COOH terminus contains struc-

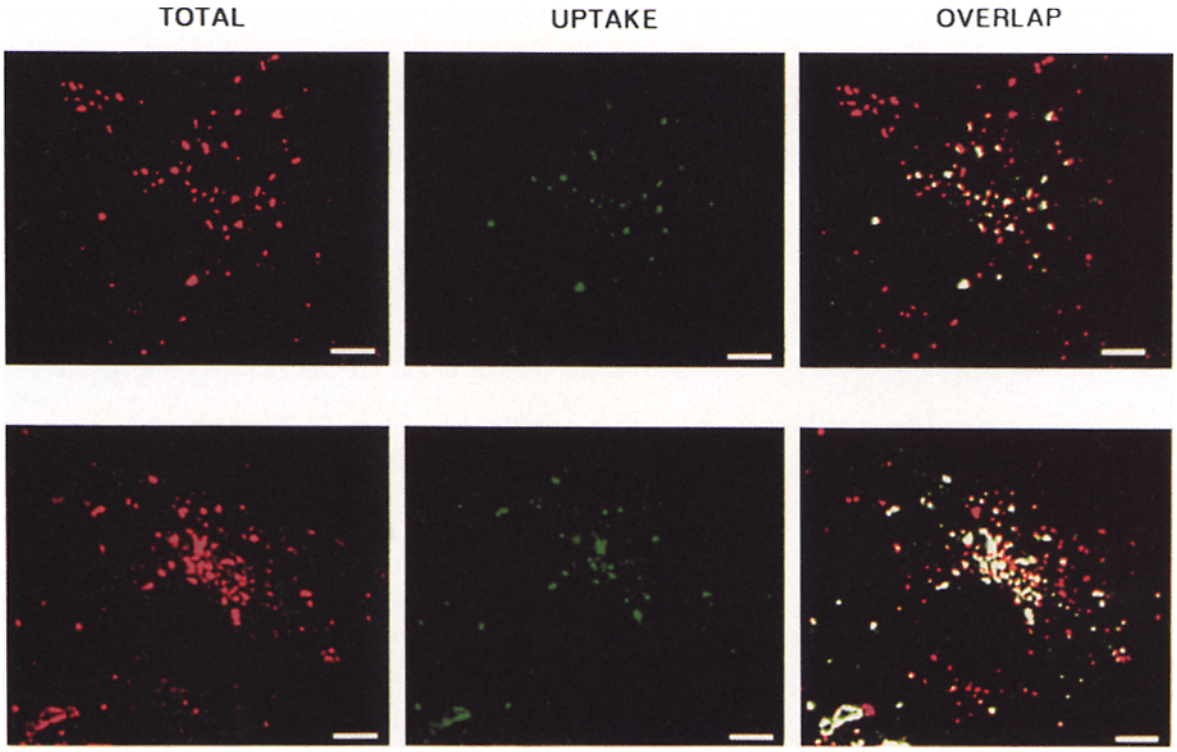

Figure 7. Colocalization of internalized antibody and expressed transporter 1(1-462)/4 in transiently transfected COS-7 cells. 48 h after transfection, cells were incubated in anti-HA IgG for 60 min at 37°C. The cells were washed on ice with acidic buffer and fixed in 4% formaldehyde. Permeabilized cells were then incubated with FITC-conjugated anti-mouse antibody (*green*, *UPTAKE*). Total transporter expression (*red*, *TOTAL*) was analyzed as indicated in the legend of Fig. 2. Thirty two-dimensional images were taken at 0.25 μm intervals. The background was subtracted and blurring above and below the plane of focus was reversed. Images shown are single optical sections from the middle of the cell. Obvious areas of correspondence were observed in all optical planes, and the coordinates of these areas were used to overlap the images. Colocalization of signal is represented by the white areas in the OVERLAP panels. Bar, 10 μm.

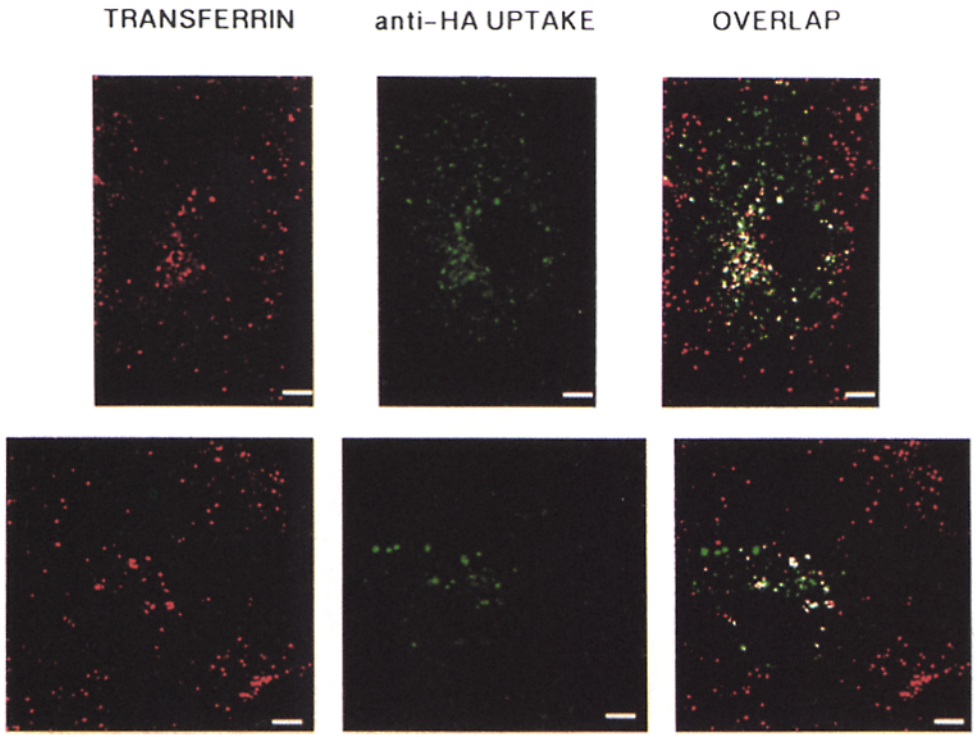

Figure 8. Colocalization of internalized anti-HA antibody and transferrin in COS-7 cells transiently expressing 1(1-462)/4. 48 h after transfection, cells were incubated with Texas red-labeled transferrin (*red*, *TRANSFERRIN*) and anti-HA IgG for 60 min. After washing with acidic buffer, fixation, and permeabilization, internalized antibody was detected with FITC-conjugated anti-mouse antibody (*green*, *UPTAKE*). Images were analyzed as described in Fig. 7. Colocalization of signal is represented by the white areas in the OVERLAP panels. Bar, 10 μm.

tural elements recognized by cells as a signal for rapid endocytosis: First, similar results are obtained when either transiently transfected COS-7 (Fig. 4) or stably transfected CHO (Fig. 5) cells were analyzed for anti-HA antibody uptake. Second, the marked stimulatory influence of the GLUT4 COOH terminus on transporter internalization is observed with both microscopic (Figs. 4 and 5) and biochemical (Fig. 6) methods. Third, an effect of the GLUT4 COOH terminus is readily measured when cells are incubated with anti-HA antibody for only two minutes, making it unlikely that later events in the membrane recycling pathway are contributing to this assay. Fourth, our assays involve binding of the same anti-HA antibody preparation to the identical HA-tagged GLUT1 domain in both GLUT1X and chimera 1(1-462)/4. Thus, it is unlikely that differences in kinetics of association of antibody with these transporter proteins contribute to the observed differences in antibody internalization rates mediated by the two transporters.

The endocytosis rate of the expressed 1(1-462)/4 chimera reported here in CHO cells agrees remarkably well with previous reports on the endocytosis rate of endogenous GLUT4 in insulin-sensitive cells. This indicates the anti-HA antibody does not effect transporter internalization rates. Thus, Fig. 6 reveals the loss of about two thirds of the initial cell surface-bound anti-HA antibody after a 10-min incubation of CHO cells at 37°C. This is virtually identical to the values reported in 3T3-L1 cells (39) and rat adipocytes (6) for fractional movement of affinity-labeled or trypsin-cleaved cell surface GLUT4 from plasma membranes to intracellular membranes, respectively, under basal conditions. In another study, affinity-labeled GLUT4 in primary fat cells was reported to be internalized at a somewhat faster rate than reported in the above studies (20). Taken together, the data are consistent with the hypothesis that the GLUT4 COOH terminus is a major signal within the GLUT4 structure that confers its characteristic rapid endocytosis rate. This hypothesis will require rigorous testing by comparing endocytosis of native GLUT4 vs chimera 1(1-462)/4 in insulin-sensitive cultured 3T3-L1 adipocytes. Appropriate transfected cell lines are currently being developed for this analysis.

In contrast to the general agreement that GLUT4 internalizes rapidly, our results suggesting a lower GLUT1 endocytosis rate is inconsistent with data published by Yang and Holman (39). These workers reported that GLUT1 was internalized as rapidly as GLUT4 in 3T3-L1 adipocytes. This discrepancy may be due to the different cell types used in their studies, or to the disparate methods used to quantify endocytosis. Yang and Holman (39) rely on affinity labeling of cell surface transporter proteins with an impermeant bismannose photolabel to follow internalization of GLUT1 and GLUT4. It has not been established that the small fraction of labeled transporters in those studies are directed into the same cellular membrane microcompartments as are the native transporters. In this regard, evidence that a large fraction of cell surface GLUT1 proteins may not be catalytically active in unstimulated 3T3-L1 adipocytes has been reported (12, 14). These suppressed transporter proteins may not react with a probe directed to their extracellular glucose binding site. Thus, affinity photolabeling may not be an appropriate method for monitoring the membrane dynamics of the total pool of GLUT1 proteins in 3T3-L1 adipocytes. Additionally, Yang and Holman (39) determine endocytosis rates indirectly using cell fractionation techniques, which might lead to results that differ from direct measurements on intact cells as reported here.

The finding that the COOH terminus of GLUT4 contains information for rapid endocytosis raises the question of whether the different steady-state subcellular localizations of GLUT4 and GLUT1 are entirely due to differences in endocytic rates of these two molecules. The present finding that GLUT1 endocytosis is relatively slow appears to explain, at least in part, this high cell surface display of GLUT1 in the basal state. The rapid endocytosis of GLUT4 would explain its predominantly intracellular distribution. However, another possibility is that a subfraction of GLUT4 transporters are targeted to a distinct intracellular membrane pool which does not cycle to and from the plasma membrane, whereas another pool, which is revealed by antibody uptake, is internalized and recycles continually to the plasma membrane. This issue was addressed by assessing the degree to which the pool of newly internalized anti-HA antibody-bound 1(1-462)/4 chimera segregated into the same cellular membrane compartments as the bulk chimera transporter proteins. This analysis showed a striking colocalization of these two transporter populations (Fig. 7). These data argue against the idea that sub-populations of GLUT4 transporters with vastly divergent trafficking characteristics coexist in the same cell, and suggest that rapid endocytosis can account for the predominantly intracellular distribution of the chimeras with the GLUT4 COOH terminus.

Glucose Transporter Endocytosis as a Target of Insulin Action

It is well established in fat and muscle cells that insulin action exerts a much more dramatic effect on GLUT4 redistribution to the cell surface compared to that of GLUT1 (15, 40). The much larger proportion of GLUT1 vs GLUT4 protein already at the cell surface membrane in unstimulated cells largely accounts for this difference. The observed rapid endocytosis rate signaled by the GLUT4 COOH terminus in these studies in turn implicates endocytosis as a potentially important point for regulation by insulin. Three recent papers report such regulation, indicating a 30–66% inhibition of GLUT4 internalization by insulin (6, 20, 39). The degree to which this effect might contribute to the overall 10–20-fold increase in GLUT4 concentration in the cell surface membrane is not resolved by the present results because we have not employed insulin-sensitive cell types. However, the rate of 1(1-462)/4 endocytosis measured in our studies implies a rate of basal exocytosis that is not rapid enough to account for insulin action if only endocytosis were inhibited by the hormone. Evidence from similar studies also suggests a major effect of insulin on the process of exocytosis or other intracellular steps in the glucose transporter membrane cycling pathway (20, 39). These considerations raise the question whether the COOH terminus of GLUT4 functions specifically at the endocytosis step of GLUT4 trafficking, or also plays a role in one or more other stages of the overall recycling pathway. Evidence in favor of the latter includes our observation that differences between internalized GLUT1 vs 1(1-462)/4 increased with time (twofold greater for the latter after 2 min vs fivefold after 10 min of anti-HA uptake in Fig. 6). Thus, transit of GLUT1 through the mem-

brane recycling pathway and back to the cell surface may be more rapid than that for GLUT4.

GLUT4 Trafficking Involves the Clathrin-coated Pit Endocytosis Pathway

Studies directed towards understanding the molecular basis of endocytosis have demonstrated that clathrin-coated pits on the cell surface membrane mediate entry of many cell surface proteins into complex intracellular membrane trafficking pathways. Recent work has focused on identifying motifs present in receptor cytoplasmic tails that govern routing through such cellular membrane systems. One such identified motif consists in the presence of one or more tyrosine residues in the juxtamembrane region of several receptor proteins (18, 36). Another cytoplasmic structural element that appears to mediate coated pit–mediated endocytosis and lysosomal targeting consists of a leucine doublet (21, 22, 25, 27, 31, 37). The presence of leucines 489 and 490, and tyrosine 504 in the COOH terminus of GLUT4 but not GLUT1 (Fig. 1 *B*) prompted our evaluation of their possible functional roles within the GLUT4 COOH-terminal domain. Mutation of the dileucine motif in the GLUT4 COOH terminus to dialanine was accompanied by loss of the rapid endocytosis rate of 1(1-462)/4, and by a parallel loss of its steady-state intracellular distribution (Figs. 4–6). In contrast, truncation of tyrosine 504 was without effect, suggesting that the dileucine motif is the key determinant of the sorting properties of the GLUT4 COOH terminus. During the final preparation of our manuscript, a report by Verhey and Birnbaum (38) appeared which also demonstrates the steady-state perinuclear distribution directed by the GLUT4 COOH terminus requires an intact double leucine motif. Importantly, the present data are consistent with the postulate that disruption of the rapid endocytosis rate by mutation of the GLUT4 COOH terminus double leucine causes the cell surface display of the mutant 1(1-462)/4LL chimera, although the abolition of other functions such as localization to a sequestered membrane compartment by the mutation may also occur.

The finding that endocytosis of the 1(1-462)/4 chimera is impaired by mutation of the double leucines to alanines also further implicates a coated-pit based mechanism for cellular internalization of this chimera. This concept derives from the fact that several other receptors that require intact dileucines for appropriate delivery of their ligands to lysosomes, including the insulin-like growth factor II (IGF-II)/mannose-6-phosphate (M6P) receptor (22), the cation-dependent M6P receptor (21), CD3 (25), and CD4 (31) polypeptides, and the lysosomal integral membrane protein II (37) appear to employ this pathway. This hypothesis gains further strong support from recent studies showing direct association of GLUT4 transporters with cell surface coated pits (30) and with isolated coated vesicles (3). Furthermore, it is well documented that the transferrin receptor is present in coated pits and is internalized by this mechanism. The 1(1-462)/4 chimera was found to colocalize with internalized transferrin upon its endocytosis in COS-7 cells (Fig. 8), indicating a common pathway of cell entry. These considerations suggest the hypothesis that one or more components associated with coated membranes may directly interact with the double leucine region of the GLUT4 COOH terminus. Identifying these hypothetical partners for the dileucine motif in GLUT4 is an important objective. A key question also raised by these studies is whether insulin action directly modulates the interaction between this GLUT4 COOH-terminal domain and cellular components involved in protein sorting and trafficking.

We thank Judy Kula for excellent assistance in preparation of the manuscript.

This work was supported by grants from the National Institutes of Health (DK30898 to M. P. Czech) and the Juvenile Diabetes Foundation International (to S. Corvera).

Received for publication 24 February 1994 and in revised form 16 May 1994.

References

1. Asano, T., K. Takata, H. Katagiri, K. Tsukuda, J.-L. Lin, H. Ishihara, K. Inukai, H. Hirano, Y. Yazaki, and Y. Oka. 1992. Domains responsible for the differential targeting of glucose transporter isoforms. *J. Biol. Chem.* 267:19636–19641.
2. Birnbaum, M. J. 1989. Identification of a novel gene encoding an insulin-responsive glucose transporter protein. *Cell.* 57:305–315.
3. Chakrabarti, R., J. Buxton, M. Joly, and S. Corvera. 1994. Insulin-sensitive association of GLUT-4 with endocytotic clathrin-coated vesicles revealed with the use of Brefeldin A. *J. Biol. Chem.* 269:7926–7933.
4. Charron, M. J., F. C. Brosius, S. L. Alper, and H. F. Lodish. 1989. A glucose transport protein expressed predominantly in insulin-responsive tissues. *Proc. Natl. Acad. Sci. USA.* 86:2535–2539.
5. Cushman, S. W., and L. J. Wardzala. 1980. Potential mechanism of insulin action on glucose transport in the isolated rat adipose cell. *J. Biol. Chem.* 255:4758–4762.
6. Czech, M. P., and J. M. Buxton. 1993. Insulin action on the internalization of the GLUT4 glucose transporter in isolated rat adipocytes. *J. Biol. Chem.* 268:9187–9190.
7. Czech, M. P., A. Chawla, C.-W. Woon, J. Buxton, M. Armoni, W. Tang, M. Joly, and S. Corvera. 1993. Exofacial epitope-tagged glucose transporter chimeras reveal COOH-terminal sequences governing cellular localization. *J. Cell Biol.* 123:127–135.
8. Czech, M. P., B. M. Clancy, A. Pessino, C.-W. Woon, and S. A. Harrison. 1992. Complex regulation of simple sugar transport in insulin-responsive cells. *Trends Biochem. Sci.* 17:197–201.
9. Davis, R. J., M. Faucher, L. K. Racaniello, A. Carruthers, and M. P. Czech. 1987. Insulin-like growth factor I and epidermal growth factor regulate the expression of transferrin receptors at the cell surface by distinct mechanisms. *J. Biol. Chem.* 262:13126–13134.
10. Fukumoto, H., T. Kayano, J. B. Buse, Y. Edwards, P. F. Pilch, G. I. Bell, and S. Seino. 1989. Cloning and characterization of the major insulin-responsive glucose transporter expressed in human skeletal muscle and other insulin-responsive tissues. *J. Biol. Chem.* 264:7776–7779.
11. Gorman, C. 1985. High efficiency gene transfer into mammalian cells. *In* DNA Cloning. D. M. Glover, editor. IRL Press, Oxford, Vol. II. 143–190.
12. Harrison, S. A., B. M. Clancy, A. Pessino, and M. P. Czech. 1992. Activation of cell surface glucose transporters measured by photoaffinity labeling of insulin-sensitive 3T3-L1 adipocytes. *J. Biol. Chem.* 267: 3783–3788.
13. Harrison, S. A., J. M. Buxton, A. L. Helgerson, R. G. MacDonald, F. J. Chlapowski, A. Carruthers, and M. P. Czech. 1990. Insulin action on activity and cell surface disposition of human HepG2 glucose transporters expressed in Chinese Hamster Ovary cells. *J. Biol. Chem.* 265: 5798–5801.
14. Harrison, S. A., J. M. Buxton, and M. P. Czech. 1991. Suppressed intrinsic catalytic activity of GLUT1 glucose transporters in insulin-sensitive 3T3-L1 adipocytes. *Proc. Natl. Acad. Sci. USA.* 88:7839–7843.
15. Harrison, S. A., J. M. Buxton, B. M. Clancy, and M. P. Czech. 1990. Insulin regulation of hexose transport in mouse 3T3-L1 cells expressing the human HepG2 glucose transporter. *J. Biol. Chem.* 265:20106–20116.
16. Holman, G. D., I. J. Kozka, A. E. Clark, C. J. Flower, J. Saltis, A. D. Habberfield, I. A. Simpson, and S. W. Cushman. 1990. Cell surface labeling of glucose transporter isoform GLUT4 by bis-mannose photolabel. *J. Biol. Chem.* 265:18172–18179.
17. Hudson, A. W., D. C. Fingar, G. A. Seidner, G. Griffiths, B. Burke, and M. J. Birnbaum. 1993. Targeting of the "insulin-responsive" glucose transporter (GLUT4) to the regulated secretory pathway in PC12 cells. *J. Cell Biol.* 122:579–588.
18. Humphrey, J. S., P. J. Peters, L. C. Yuan, and J. S. Bonifacino. 1993. Localization of TGN38 to the *trans*-Golgi network: involvement of a cytoplasmic tyrosine-containing sequence. *J. Cell Biol.* 120:1123–1135.
19. James, D. E., M. Strube, and M. Mueckler. 1989. Molecular cloning and characterization of an insulin-regulatable glucose transporter. *Nature (Lond.).* 338:83–87.

20. Jhun, B. H., A. L. Rampal, H. Liu, M. Lachaal, and C. Y. Jung. 1992. Effects of insulin on steady state kinetics of GLUT4 subcellular distribution in rat adipocytes. *J. Biol. Chem.* 267:17710-17715.
21. Johnson, K. F., and S. Kornfeld. 1992. A His-Leu-Leu sequence near the carboxyl terminus of the cytoplasmic domain of the cation-dependent Mannose-6-phosphate receptor is necessary for the lysosomal enzyme sorting function. *J. Biol. Chem.* 267:17110–17115.
22. Johnson, K. F., and S. Kornfeld. 1992. The cytoplasmic tail of the mannose-6-phosphate/insulin-like growth factor-II receptor has two signals for lysosomal enzyme sorting in the Golgi. *J. Cell Biol.* 119: 249–257.
23. Kaestner, K. H., R. J. Christy, J. C. McLenithan, L. T. Braiterman, P. Cornelius, P. H. Pekala, and M. D. Lane. 1989. Sequence, tissue distribution, and differential expression of mRNA for a putative insulin-responsive glucose transporter in mouse 3T3-L1 adipocytes. *Proc. Natl. Acad. Sci. USA.* 86:3150–3154.
24. Kanai, F., Y. Nishioka, H. Hayashi, S. Kamohara, M. Todaka, and Y. Ebina. 1993. Direct demonstration of insulin induced GLUT4 translocation to the surface of intact cells by insertion of a c-myc epitope into an exofacial GLUT4 domain. *J. Biol. Chem.* 268:14523–14526.
25. Letourneur, F., and R. D. Klausner. 1992. A novel di-leucine motif and a tyrosine based motif independently mediate lysosomal targeting and endocytosis of CD3 chains. *Cell.* 69:1143–1157.
26. Marshall, B. A., H. Murata, R. C. Hresko, and M. Mueckler. 1993. Domains that confer intracellular sequestration of the GLUT4 glucose transporter in *Xenopus* oocytes. *J. Biol. Chem.* 268:26193–26199.
27. Mori, S., L. Claesson-Welsh, and C.-H. Heldin. 1991. Identification of a hydrophobic region in the carboxyl terminus of the platelet-derived growth factor β-receptor which is important for ligand-mediated endocytosis. *J. Biol. Chem.* 266:21158–21164.
28. Oka, Y., and M. P. Czech. 1984. Photoaffinity labeling of insulin-sensitive hexose transporters in intact rat adipocytes. *J. Biol. Chem.* 259:8125–8133.
29. Piper, R. C., C. Tai, J. W. Slot, C. S. Hahn, C. M. Rice, H. Huang, and D. E. James. 1992. The efficient intracellular sequestration of the insulin-regulatable glucose transporter (GLUT-4) is conferred by the NH_2 terminus. *J. Cell Biol.* 117:729–743.
30. Piper, R. C., C. Tai, P. Kulesza, S. Pang, D. Warnock, J. Baenziger, J. W. Slot, H. J. Geuze, C. Puri, and D. E. James. 1993. GLUT-4 NH_2 terminus contains a phenylalanine-based targeting motif that regulates intracellular sequestration. *J. Cell Biol.* 121:1221–1232.
31. Shin, J., R. L. Dunbrack, Jr., S. Lee, and J. L. Strominger. 1991. Phosphorylation-dependent down-modulation of CD4 requires a specific structure within the cytoplasmic domain of CD4. *J. Biol. Chem.* 266:10658–10665.
32. Simpson, I. A., and S. W. Cushman. 1986. Hormonal regulation of mammalian glucose transport. *Annu. Rev. Biochem.* 55:1059–1089.
33. Slot, J. W., H. J. Geuze, S. Gigengack, G. E. Lienhard, and D. E. James. 1991. Immunolocalization of the insulin regulatable glucose transporter in brown adipose tissue of the rat. *J. Cell Biol.* 113:123–135.
34. Smith, R. M., M. J. Charron, N. Shah, H. F. Lodish, and L. Jarrett. 1991. Immunoelectron microscopic demonstration of insulin-stimulated translocation of glucose transporters to the plasma membrane of isolated rat adipocytes and masking of the carboxyl-terminal epitope of intracellular GLU4. *Proc. Natl. Acad. Sci. USA.* 88:6893–6897.
35. Suzuki, K., and T. Kono. 1980. Evidence that insulin causes translocation of glucose transport activity to the plasma membrane from an intracellular storage site. *Proc. Natl. Acad. Sci. USA.* 77:2542–2545.
36. Vaux, D. 1992. The structure of an endocytosis signal. *Trends Cell Biol.* 2:189–192.
37. Vega, M. A., F. Rodriguez, B. Segui, C. Cales, J. Alcalde, and I. V. Sandoval. 1991. Targeting of lysosomal integral membrane protein LIMP II. *J. Biol. Chem.* 266:16269–16272.
38. Verhey, K. J., and M. J. Birnbaum. 1994. A Leu-Leu Sequence is essential for COOH-terminal targeting signal of GLUT4 glucose transporter in fibroblasts. *J. Biol. Chem.* 269:2353–2356.
39. Yang, J., and G. D. Holman. 1993. Comparison of GLUT4 and GLUT1 subcellular trafficking in basal and insulin-stimulated 3T3-L1 cells. *J. Biol. Chem.* 268:4600–4603.
40. Zorzano, A., W. Wilkinson, N. Kotliar, G. Thoidis, B. E. Wadzinkski, A. E. Ruoho, and P. F. Pilch. 1989. Insulin-regulated glucose uptake in rat adipocytes is mediated by two transporter isoforms present in at least two vesicle populations. *J. Biol. Chem.* 264:12358–12363.